XLVI CILAMCE
VITÓRIA - ES - BRAZIL - 2025
XLVI IBERO-LATIN AMERICAN CONGRESS ON COMPUTATIONAL METHODS IN ENGINEERING

Influence of Nucleus Pulposus Geometry on FEM Simulation Results of the Lumbar Spine

João P. Schmitz[1], Emilio G. F. Mercuri[1], Aref K. L. Kzam[2]

[1]*Dept. of Numerical methods in engineering, University Federal of Paraná*
Av. Cel. Francisco H. dos Santos, 100 - Jardim das Américas, Curitiba, 81530-000, Paraná, Brazil, joao.schmitz.eng@gmail.com, emiliomercuri@gmail.com
[2]*Dept. of Infrastructure and territory, University Federal of Latin American Integration*
Av. Tarquinio Joslin dos Santos, 1000, Polo Universitario, Foz do Iguaçu, 85870-650, Paraná, Brazil, Aref.kzam@unila.edu.br

Abstract. The lumbar spine is a critical region due to its high incidence of pain and injuries. This study investigates the influence of nucleus pulposus (NP) size and positioning on the biomechanical behavior of the intervertebral disc (IVD) through finite element analysis (FEA). Two models (L4-S1) were developed: Model 1 (M1) followed Kapandji's parameters (NP occupying 27% of the IVD, positioned posteriorly), while Model 2 (M2) adopted a larger (40%) and more centralized NP based on recent literature. Both models were simulated in ANSYS Mechanical Pro 17.0 under vertical loads (300 N) and moments (7.5 N·m) to assess stress distribution and strain. Results showed that M2 exhibited a load distribution closer to in vivo data, with ~75% of stresses concentrated in the NP, aligning with Kapandji's theoretical values. In contrast, M1 displayed uneven stress sharing, particularly during extension (61.4% NP load) and flexion (53.5% AF load). Strain analysis further confirmed M2's biomechanical superiority, though both models were limited by simplifications.

Keywords: Lumbar spine, finite element analysis, intervertebral disc, nucleus pulposus, biomechanics.

1 Introduction

The lumbar region of the vertebral column is a critical area for studies due to its high incidence of pain and injuries Wilke [1]. The complexity of the vertebral column stems from its various constituent elements, including five larger vertebral bodies with more developed articular processes Appel [2]. Between the vertebral bodies, the intervertebral discs (IVDs) consist of the annulus fibrosus (AF), nucleus pulposus (NP), and cartilaginous endplate (CEP), along with other elements such as ligaments, articular process cartilage, and muscles Moore [3].

According to Hamill [4], the most complex region is the IVD, as the NP has fluid-like characteristics due to its composition and is encapsulated by concentric layers of the AF. These AF layers contain collagen fibers arranged at angles varying from 30 to 120 degrees, oriented perpendicularly between adjacent layers Hamill [5].
Computational simulations have become essential tools for understanding the biomechanical behavior of this region, enabling analysis of stresses, displacements, and loads under various conditions, as demonstrated by Goto [6] and Mollica [7]. Models vary in complexity, ranging from simplified representations of vertebrae and IVDs to more detailed models incorporating ligaments, muscles, and articular facets Xu [8].
Several parameters influence lumbar simulation results. Among the most relevant are the mechanical properties of the IVD, which can be represented in various ways, including elastic Lu [9] and hyperelastic properties Ardatov [10].
The geometric complexity of the IVD also varies, with features such as the number of AF layers (with or without fibers), NP size and positioning, and different representations of articular process connections. These modeling variations can lead to significant changes in results Li [11].
To clarify the influence of NP size and positioning, we compare two models of the L4-S1 region (fourth lumbar

vertebra to first sacral vertebra) with distinct NP characteristics. Model 1 (M1) has an NP occupying 27% of the IVD, positioned 2/10 from the posterior and 4/10 from the anterior region, following Kapandji [12] parameters. Model 2 (M2) has an NP occupying 40% of the IVD, positioned more centrally according to recent studies. Simulations were performed using ANSYS [13] and the finite element method (FEM) to analyze both models' responses. By examining result variations between the models, we can determine which geometric characteristics better align with in vivo data.

.

2 Metodology

The model was generated using the open-access program 3D Slicer [14], along with a magnetic resonance imaging (MRI) scan obtained from the USP database. The scan was from a healthy lumbar region of a woman of unknown age and approximately 60 kg in weight.

The model Figure 1a was corrected and segmented into its respective structures—lumbar vertebrae 4 and 5 (L4, L5), sacral vertebra 1 (S1), nucleus pulposus (NP) and annulus fibrosus (AF) of L4-L5, as well as NP and AF of L5-S1—using Ansys SpaceClaim.

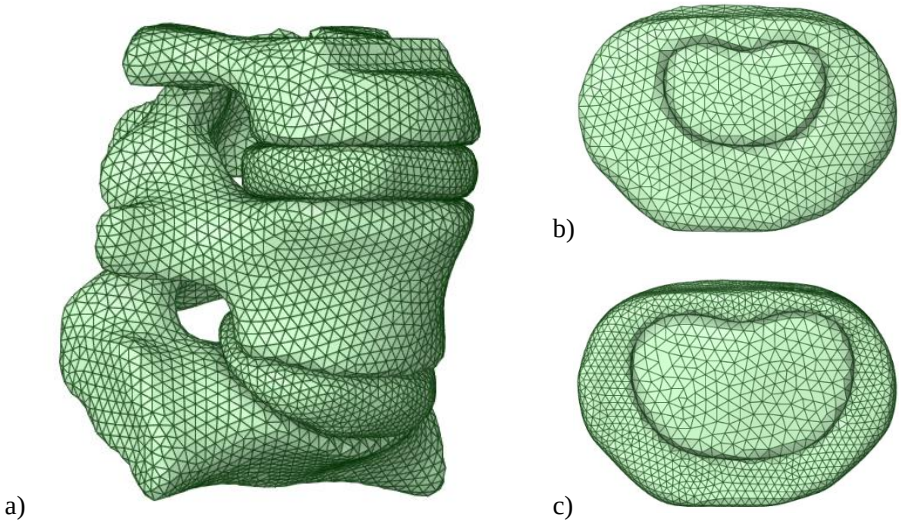


Figure 1. a) Model complete L4-S1; b) IDV Model 1; c) IDV Model 2

At this stage, the two model types were created: the model 1 (M1) with an NP occupying 27% of the IVD volume and positioned according to Kapandji [12] specifications (4/10 of the anterior region and 2/10 of the posterior region) Figure 1b, while the model 2 (M2) was created with an NP occupying 40% of the volume and positioned at 2/10 of the posterior region Figure 1c. The second model features an NP size more consistent with recent studies that establish the NP as approximately 40-50% of the IVD volume Bashkuev [15], Du [16], Qasim [17], Von Forvel [18]. Both models were simulated without the cartilaginous endplate.

Then, after a statistical analysis of data from studies of Rodrigues [19] which compiled more than 30 articles with elastic properties used to characterize IVD components, the median values were selected. For the NP, this resulted in properties of 1 MPa for the elastic modulus and 0.499 for Poisson's ratio.

For the AF, which consists of two structural components (fibrous layers and viscous substance), the selected properties were:

- Fibrous layers: 450 MPa elastic modulus and 0.3 Poisson's ratio.
- Viscous substance: 4.2 MPa elastic modulus and 0.499 Poisson's ratio.

Using the rule of mixtures, these two AF phases were combined into a single element. The properties of this new element were manually calibrated based on the internal NP pressure parameters obtained from in vitro tests from Brinckmann and Grootenboer [20] under a 300N vertical load, the model M2 was used for this calibration.The final calibrated properties were:

- Elastic modulus: 10 MPa.
- Poisson's ratio: 0.45.

The mixture ratio was determined as 1.3% fibrous layers and 98.7% viscous substance. These same properties were applied to M1 and M2.

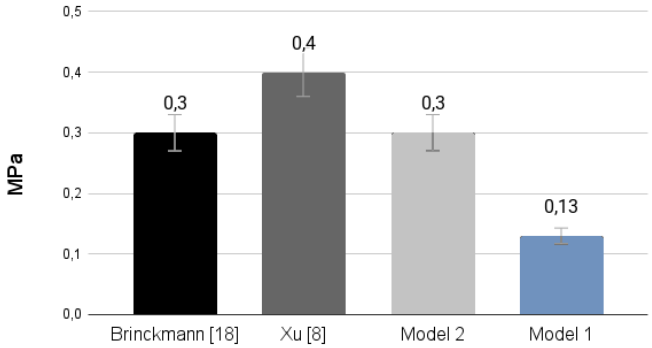


Figure 2. Mean stress in the nucleus pulposus

The next step was configuring the connections between model elements. The vertebral bodies (L4, L5 and S1) in contact with the AF and NP were considered perfectly bonded without slip, ensuring uniform load and movement transfer between components. The connections between vertebral bodies at the articular processes were modeled as cylindrical joints allowing rotation about the axis and small axial displacements. The base of the S1 vertebral body was fixed as it has no natural movement.

The mesh was then refined with the following specifications:

- Low-interest regions (vertebral bodies L4, L5, S1 and L5-S1 IVD): 3.5 mm and 2.5 mm elements respectively;
- Contact surfaces between L4/L5 vertebrae and L4-L5 IVD: 1 mm elements;

For the target IVD (L4-L5), a mesh convergence test was performed using 4-node tetrahedral elements solid 285, ranging from 5 mm to 0.7 mm. The final element sizes were set to 1.5 mm for M1 and 1 mm for M2, based on both element quality and results variation below 5%.

With these configurations established, loading conditions were applied based in the data of Xu [8]:

- Vertical load: 300 N
- Moments: 7.5 N·m

The moments were applied simultaneously with vertical loading to simulate:

- Axial rotation (both directions)
- Flexion
- Extension
- Lateral bending (both directions)

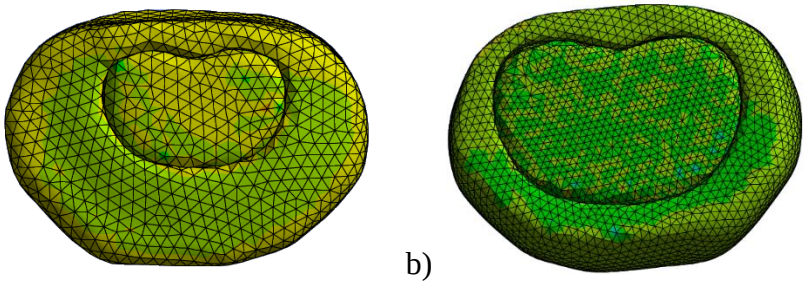


Figure 3. Stress distribuition in the IDV. a) Model 1 vertical load; b) Model 2 Flexion and vertical load

For the initial comparison between models M1 and M2, the analyzed results were maximum principal strains and average principal stresses. Examining Model 1 first, the Table 1 shows that except for extension and flexion, the average stress in the AF and NP are quite similar despite differences in size and mechanical properties of the elements, indicating uniform load distribution during rotation, lateral bending, and pure vertical loading.

During extension, in Model 1 the NP receives approximately 61.4% of the stress reaching the IVD, showing that during this movement the posterior IVD region is overloaded, and since the NP is located closer to this region, it ends up receiving more stress. In flexion, the AF is more overloaded, receiving 53.5% of the load reaching the IVD, as the NP is displaced posteriorly.

Table 1. Mean Principal Compression Stress In The Intervertebral Disc

Element	Mean Rotation (MPa)	Extension (MPa)	Flexion (MPa)	Mean Lateral Bending (MPa)
M1 - AF	0.13	0.037	0.23	0.14
M1 - NP	0.13	0.059	0.20	0.13
M2 - AF	0.12	0.11	0.12	0.11
M2 - NP	0.19	0.4	0.2	0.3

Now analyzing the datas of M2 on Table 1, we observe that compressive stresses reaching the IVD are primarily directed to the NP, since it occupies 40% of the disc volume. During extension, the NP carries 78.4% of the total IVD stress. For rotation and flexion, both components bear approximately 60% of the stress, while during lateral bending and vertical loading, the NP sustains 73.2% of the compressive stress reaching the IVD.

The maximum principal strain results Table 2 show similar patterns between NP and AF during rotation, lateral bending and vertical loading, with the NP exhibiting about 2% greater strain.

However, during extension this relationship reverses, with the AF showing approximately 2% higher strain. Under flexion loading, the NP demonstrates significantly greater deformation - up to 23% higher than the annulus fibrosus.

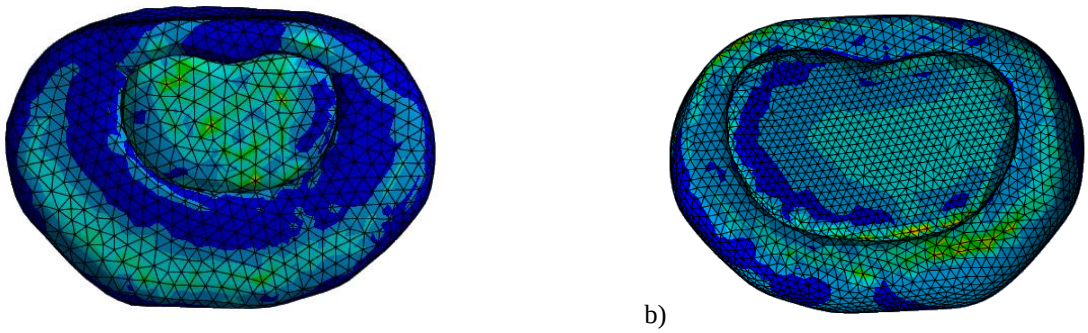
Table 2. Maximum Principal Strain in the Intervertebral Disc

Element	Mean Rotation mm/mm	Extension mm/mm	Flexion mm/mm	Mean Lateral Bending mm/mm	Vertical Load mm/mm
M1 - AF	0,15	0,21	0,15	0,15	0,15
M1 - NP	0,17	0,20	0,24	0,16	0,16
M2 - AF	0,4	0,69	0,50	0,21	0,2
M2 - NP	0,51	0,81	0,54	0,42	0,38

The deformations in M2, presented in Table 2, show variations that follow the stress distribution pattern, with higher values in the NP. During rotation, deformations are 12% greater in the NP. In extension, the AF shows 8% less deformation, while in flexion, the NP deformation is only 3.85% greater. For lateral bending and vertical loading alone, the NP deformation shows approximately 32% greater variation.

According to Kapandji [12], loads reaching the IVD are distributed in a 75%-25% proportion between NP and AF respectively. Considering this, M2 demonstrates a distribution closer to Kapandji's stipulated values, even though M1 was developed following NP positioning parameters (2/10 and 4/10).

Another noteworthy point is that the absence of cartilaginous endplates leads to uneven stress distribution. Additional factors affecting this distribution include: the natural asymmetry of IVDs generated from real imaging exams, and computational limitations that constrained tetrahedral element size, resulting in stress/deformation outliers as visible in the Figure 4 a) and b).



a) b)

Figure 4. Maximum Strain in the Intervertebral Disc a) Model 1 mesh size 1,5mm; b) Model 2 mesh size 1mm.

3 Conclusions

From these results, we can observe that although M1 follows Kapandji's geometric standards for nucleus positioning, Model 2 demonstrates load distribution characteristics that better approximate the stress patterns reported in Xu and Brinckmann models in the vertical loading studies.

The moment analyses showed favorable trends, with approximately 75% of loads being directed to the NP in M2 - closely matching theoretical expectations.

However, M2 still requires refinements and the next steps include:

- Slight anterior repositioning of the NP in Model 2;
- Implementation of superior and inferior cartilaginous endplates to improve load distribution;
- Testing of alternative configurations for the articular processes;
- Enhanced modeling of the annulus fibrosus complexity through separate representation of collagen fiber layers and ground substance;
- Evaluation of hyperelastic properties and fluid-like behavior in the nucleus pulposus.

Acknowledgements. The authors would like to thank the support of the Brazilian research agencies CAPES (Coordination for the Improvement of Higher Education Personnel) and CNPq (National Council for Scientific and Technological; grant309515/2017-3). And UFPR Federal University of Paraná, and UNILA (Federal University of Latin American Integration).

Authorship statement. The authors here by confirm that they are the soleliable persons responsible for the authorship of this work, and that all material that has been here in included as part of the presente paper is either the property (and authorship) of the authors, or has the permission of the owners to be included here**.**

References

[1] Wilke, Hans-Joachim, et al. "Intradiscal pressure together with anthropometric data–a data set for the validation of models." Clinical biomechanics 16 (2001): S111-S126.
[2] Appel, Fernando. Coluna vertebral: conhecimentos básicos. In: Coluna vertebral: conhecimentos básicos. 2002. p. 151-151.
[3] Moore, Keith L.; DALLEY, Arthur F.; AGUR, Anne MR. Clinically Oriented anatomy. Lippincott Williams & Wilkins, 2013.
[4] Hamill, J.; Bates, B. T. A kinetic evaluation of the effects of in vivo loading on running shoes. Journal of Orthopaedic & Sports Physical Therapy, v. 10, n. 2, p. 47-53, 1988. DOI 10.2519/jospt.1988.10.2.47.
[5] Hamill, J.;Knutzen,K. Bases Biomecânicas do Movimento Humano. 4. ed. Barueri: Manole, 2016, 315p.

[6] Goto, K. et al. Mechanical analysis of the lumbar vertebrae in a three-dimensional finite element method model in which intradiscal pressure in the nucleus pulposus was used to establish the model. Journal of orthopaedic science, v. 7, n. 2, p. 243-246, 2002.
[7] Mollica, Caterina et al. Augmented Reality Surgical Navigation (ARSN) for percutaneous pedicle screw placement in thoracic and lumbar spine: results from a multicentric prospective study. Brain and Spine, v. 2, p. 101681, 2022. [s.l: s.n.]. DOI 10.1016/j.bas.2022.101681.
[8] Xu, Ming, et al. "Lumbar spine finite element model for healthy subjects: development and validation." Computer methods in biomechanics and biomedical engineering 20.1 (2017): 1-15.
[9] Lu, X. et al. Biomechanical effects of interbody cage height on adjacent segments in patients with lumbar degeneration: a 3D finite element study. Journal of orthopaedic surgery and research, v. 17, n. 1, p. 325, 2022. DOI 10.1186/s13018-022-03220-3.
[10] Ardatov, Oleg et al. Modeling the Effect of Annulus Fibrosus Stiffness on the Stressed State of a Vertebral L1 Body and Nucleus Pulposus. Bioengineering, v. 11, n. 4, p. 305, 2024.
[11] Li, Quan You et al. Biomechanical analysis of lumbar decompression surgery in relation to degenerative changes in the lumbar spine–Validated finite element analysis. Computers in biology and medicine, v. 89, p. 512-519, 2017.
[12] Kapandji, A. I. Fisiologia articular–tronco e coluna vertebral. Vol 3. 5. Ed. Paris: Editions Maloine. 2000. 248p.
[13] ANSYS Mechanical Pro. Versão 2017. Canonsburg, PA: ANSYS Inc.
[14] 3D SLICER. Versão 5.6.1. Boston: The Slicer Community, 2023.
[15]Bashkuev, Maxim; Reitmaier, Sandra; Schmidt, Hendrik. Relationship between intervertebral disc and facet joint degeneration: a probabilistic finite element model study. Journal of biomechanics, v. 102, p. 109518, 2020.
[16] Du, Cheng-Fei et al. Does oblique lumbar interbody fusion promote adjacent degeneration in degenerative disc disease: A finite element analysis. Computers in biology and medicine, v. 128, p. 104122, 2021.
[17] Qasim, Muhammad et al. Damage accumulation location under cyclic loading in the lumbar disc shifts from inner annulus lamellae to peripheral annulus with increasing disc degeneration. Journal of biomechanics, v. 47, n. 1, p. 24-31, 2014.
[18] Von Forell, Gregory A. et al. Low back pain: a biomechanical rationale based on “patterns” of disc degeneration. Spine, v. 40, n. 15, p. 1165-1172, 2015.
[19] RODRIGUES, M. Análise e projecto de estruturas para substituição do disco intervertebral, 2012. Dissertação (Mestrado em Engenharia Mecânica e industrial) Faculdade de ciências e tecnologia, Universidade Nova.
[20] Brinckmann, Paul, and Henk Grootenboer. "Change of disc height, radial disc bulge, and intradiscal pressure from discectomy an in vitro investigation on human lumbar discs." Spine 16.6 (1991): 641-646.